

## The March 1997 Westerly Wind Event and the Onset of the 1997/98 El Niño: Understanding the Role of the Atmospheric Response

MATTHIEU LENGAINNE, JEAN-PHILIPPE BOULANGER, CHRISTOPHE MENKES, GURVAN MADEC,  
AND PASCALE DELECLUSE

*Laboratoire d'Océanographie Dynamique et de Climatologie (CNRS/UPMC/IRD), Université Pierre et Marie Curie, Paris, France*

ERIC GUILYARDI AND JULIA SLINGO

*Center for Global Atmospheric Modelling, Department of Meteorology, University of Reading, Reading, United Kingdom*

(Manuscript received 4 October 2002, in final form 3 March 2003)

### ABSTRACT

In a previous study, the effect of the March 1997 Westerly Wind Event (WWE) on the evolution of the tropical Pacific Ocean was studied using an ocean general circulation model (GCM). The response was characterized by (i) a cooling of the far western Pacific ( $\sim 0.8^{\circ}\text{C}$ ), (ii) a rapid eastward displacement of the warm pool (2000 km in a month), and (iii) a weak warming of the central eastern Pacific along the path of the oceanic Kelvin wave, excited by the WWE ( $\sim 0.5^{\circ}\text{C}$ ). In this study, the atmospheric response to these aspects of the sea surface temperature (SST) response are investigated using an atmospheric GCM forced with the SST anomalies from the ocean-only experiments.

The results have demonstrated that the three aspects of the SST anomaly field, generated by the WWE, themselves initiate two types of atmospheric response, both of which favor a rapid growth toward El Niño conditions. First, the eastward displacement of the warm pool, together with the reduction of the east–west SST gradient along the forced oceanic Kelvin wave path, results in a weakening of the trade winds in the central eastern Pacific. Second, the eastward displacement of the warmest water from the western to the central Pacific, giving rise to a cooling in the far western Pacific, induces an eastward shift of convection that consequently promotes the occurrence of further frequent and intense WWEs in the following months. The characteristics of these later WWEs are controlled both by the eastward extension of the warm pool and by the SST gradients established in the far western Pacific.

The implications of these results for the onset of the 1997/98 El Niño have been considered, with the conclusion that the intense March WWE strongly contributed to the early onset and rapid growth rate of the 1997/98 El Niño, not only by its direct impact on the ocean, but also by the atmospheric variability induced by the oceanic changes that developed following this event.

### 1. Introduction

The intraseasonal zonal wind activity over the western Pacific is thought to act as a triggering mechanism for El Niño–Southern Oscillation (ENSO) warm events (Lau and Chan 1986; Kessler and Kleeman 2000). A large part of this intraseasonal activity is referred to as westerly wind events (WWEs). They occur preferentially in the boreal fall–winter season and are often connected to active phases of the Madden Julian oscillation (MJO; Madden and Julian 1994). It has been hypothesized that these WWEs, through the generation of equatorial downwelling Kelvin waves, could be a key ingredient for both El Niño timing and amplitude (Wyrtki

1985; Kessler et al. 1995; Kleeman and Moore 1997; Matsuura and Iizuka 2000). Support for this hypothesis has increased following the 1997/98 El Niño, the strongest on record. This was characterized by exceptionally strong WWEs during the 1996/97 winter in association with intense MJOs (e.g., Hendon et al. 1999; Slingo et al. 1999), leading McPhaden and Yu (1999) to speculate that this westerly wind activity was responsible for the timing and amplitude of the event. The growing phase of the 1997/98 El Niño event was particularly rapid, with an extremely steep rise in the central and eastern Pacific sea surface temperatures (SST) during March to June 1997. This was coincident with the strongest of these WWEs in terms of intensity (up to  $0.2 \text{ N m}^{-2}$ ), fetch (more than  $30^{\circ}$  longitude), and duration (about a month, from mid-February to mid-March; Fig. 1).

To explore the potential influence of the March 1997 WWE on the El Niño onset, Lengaigne et al. (2002) investigated the basin-scale ocean response to this

---

*Corresponding author address:* Dr. Matthieu Lengaigne, LODYC, Université Pierre et Marie Curie, Tour 26, 4ème étage, 4, Place Jussieu, Paris, Cedex 05 75252, France.  
E-mail: mllod@ipsl.jussieu.fr

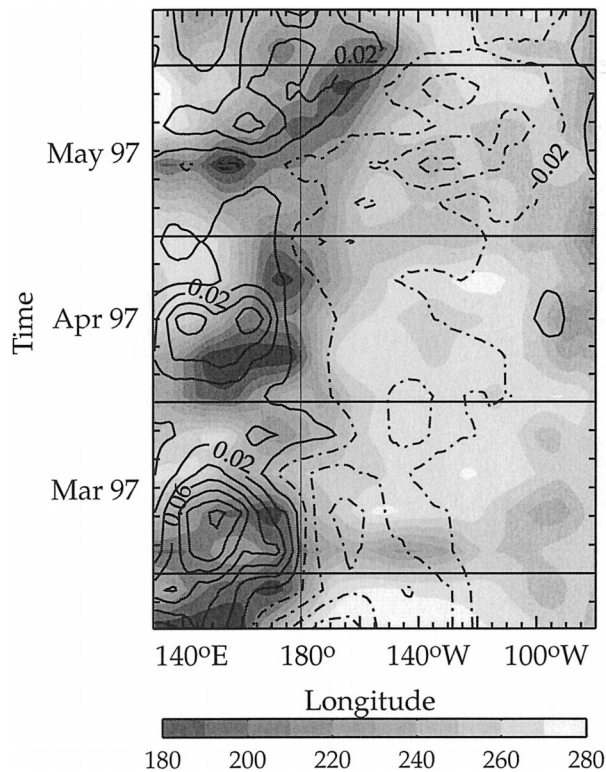


FIG. 1. Equator-time plot of observed zonal wind stress from ERS scatterometers (contours) and OLR from NOAA polar-orbiting satellites (shading) averaged over 3°N–3°S. Contour interval is 0.02 N m<sup>-2</sup>.

WWE using the Océan Parallélisé (OPA) ocean general circulation model (Madec et al. 1998) forced with observed wind stresses derived from European Remote Sensing Satellites (ERS) scatterometer measurements (Bentamy et al. 1996). Their results highlighted three oceanic responses that were extensively validated against oceanic observations. First, the WWE forced a strong downwelling Kelvin wave, which depressed the thermocline and generated an SST warming of around 0.5°C in the central and eastern Pacific through zonal temperature advection along the east–west temperature gradient. Second, this wind event was responsible for the surface advection of cold waters from near 5°N, 130°E, leading to a cooling of the far western equatorial Pacific by up to 0.8°C. Third, the nonlinear interaction between the wind-forced surface jet and the local, thermohaline front generated large zonal surface currents at the eastern edge of the warm and fresh pool (EWP), which rapidly advected the warm pool from the western to the central Pacific (2000 km in less than a month). These results highlighted therefore the strong oceanic influence of this event on the 1997/98 El Niño onset.

To go deeper in the analysis, this paper explores the response of the atmosphere to each of these three oceanic impacts in order to investigate potential positive feedback loops, which may have been responsible for

generating the largest El Niño of the twentieth century (McPhaden 1999; Boulanger and Menkes 1999; Bergman et al. 2001). Since ocean–atmosphere coupling is quite intense over the warm waters of the western equatorial Pacific, the fast displacement of the front, together with the cooling in the western Pacific, is likely to contribute significantly to the migration of the main area of convection eastward and to the persistence of westerly wind anomalies near 160°E as observed in April–May 1997 (Fig. 1). These subsequent westerly wind anomalies have been shown to be important features of the El Niño growing phase (van Oldenborgh 2000). The aim of the present study is therefore to complete the previous oceanic analysis by assessing the atmospheric response to the SST anomalies generated by the March 1997 WWE using an atmospheric GCM (AGCM). Although the focus of this study is the 1997/98 ENSO, the displacement of the warm pool during the growing phase of El Niño is characteristic of other events, suggesting that the processes and atmosphere–ocean interactions discussed in this paper may have more general relevance to our understanding of the evolution and predictability of El Niño.

The paper is organized as follows. In section 2, we briefly discuss the atmospheric model used in this study and the experimental design. Section 3 describes the atmospheric response to the oceanic effect of the March 1997 WWE, while the mechanisms involved in this response and the implication with regard to the ENSO cycle is discussed in section 4. Section 5 offers a summary and conclusions.

## 2. Description of the model and experiments

The numerical model used in this study is the atmospheric version of the Met Office Unified Model (UM), HadAM3 (Hadley Centre Atmospheric Model version 3). A detailed description of the components of the model and its performance in Atmospheric Model Intercomparison Project (AMIP)-type integrations can be found in Pope et al. (2000) and references therein. Inness and Gregory (1997) have already performed a detailed analysis of the ability of HadAM3 to simulate aspects of tropical intraseasonal activity, associated, in particular, with the Madden–Julian oscillation.

The model is run with a horizontal resolution of 2.5° latitude × 3.75° longitude, and with 19 levels in the vertical, corresponding to a layer thickness of about 100 hPa in the midtroposphere, but with higher resolution in the boundary layer and around the tropopause. Due to the nature of this study, it is worth summarizing the convection scheme here. It is the mass-flux scheme of Gregory and Rowntree (1990) including a representation of convective downdrafts (Gregory and Allen 1991) and the vertical transport of momentum by convection (Gregory et al. 1997). Convection is initiated as a parcel with a prescribed small buoyancy excess (equivalent to 0.2 K), and the initial mass flux is determined from the

buoyancy excess of the parcel after lifting from initiation level to the next level. The quality of the model's simulation of El Niño events has been studied extensively by Spencer and Slingo (2003), who showed that in the Tropics, the UM displays considerable skill in capturing the precipitation and large-scale circulation response to El Niño SST anomalies.

A series of 10-member ensemble integrations has been conducted with this AGCM from December 1996 to the end of June 1997 to investigate the atmospheric response to the SST anomalies generated by the March 1997 WWE. Each set of integrations differed only in their prescribed SSTs, which originated from the oceanic simulations performed by Lengaigne et al. (2002). To isolate the oceanic response to the WWE of March 1997, they conducted two experiments with an ocean GCM (OGCM) forced with the observed surface wind stresses for 1997 and interannual National Centers for Environmental Prediction (NCEP) heat fluxes. In the first experiments, hereafter denoted as REF, the OGCM was forced with the observed *ERS-1* and *ERS-2* weekly wind stresses, whereas in the second experiment, hereafter denoted as NWE, the OGCM was forced with the same ERS wind forcing except that the March 1997 WWE was excluded (the heat and freshwater fluxes are exactly the same in both experiments in order to focus on the dynamical impact of the WWE). Consequently the SST anomalies produced by these two forced oceanic experiments have been used as the boundary conditions for the AGCM. The control atmospheric ensemble run (named hereafter the REF ensemble run) was therefore performed using the SSTs from the reference oceanic run (REF) as boundary conditions (Fig. 2a), whereas the perturbed ensemble run (hereafter the NWE ensemble run) was performed using SSTs from the NWE oceanic run (Fig. 2b). All the members of both ensembles were initialized on 1 December 1996, keeping the ocean initial conditions constant, but taking 10 successive model days for the atmospheric initial states. The atmospheric initial conditions were generated by running the model forward for 10 days, and then taking the atmospheric initial states at the end of each day.

We restrict our diagnosis to the months from March through June 1997 for two reasons. First, by initializing 3 months prior to this period, all memory of the initial conditions is lost. Second, since the atmospheric forcing remained the same after the March WWE in the REF and NWE OGCM experiments (Lengaigne et al. 2002), the NWE ocean state tended to drift back toward the REF ocean state within a few months (after 8 months, both runs are almost identical). This means that it is not reasonable to study the atmospheric response to the REF and NWE SSTs over too long a period.

In the following discussion, the model results have been evaluated against a range of observational data. These include weekly surface wind stress data derived from the *ERS-1* and *ERS-2* scatterometers (Bentamy et al. 1996), weekly SST data from Reynolds and Smith

(1994), and pentad mean outgoing longwave radiation (OLR) data from the National Oceanic and Atmospheric Administration (NOAA) polar-orbiting satellites (Liebmann and Smith 1996). OLR from the model and observations have been used as a proxy for deep tropical convection. For compatibility with the other observational datasets, the OLR data were interpolated to weekly values; all these fields were linearly interpolated onto the AGCM grid.

### 3. Results

#### a. Convective response to the March 1997 WWE

The time evolution of REF and NWE OLR ensemble averages are presented in Fig. 2 along the equator. The most significant convective response to the SST anomalies occurs over the warm pool, a region of deep tropical convection. First, there is a strong increase in convective activity (characterized by low OLR) from mid-March to mid-June along the positive SST anomaly generated by the eastward displacement of the warm pool eastern edge (Fig. 2d). Second, the far western oceanic cooling is associated with reduced convection west of 150°E. These convective anomalies can be understood as follows. As the SST forcing of the NWE ensemble run does not include the ocean response to the March 1997 WWE, warm SSTs (>29°C) remain mostly west of the date line during the following months. Thus, deep convection ( $OLR < 230 \text{ W m}^{-2}$ ) occurs over the far western Pacific, primarily west of 160°E (Fig. 2b). In contrast, in the REF ensemble run, whose SST forcing includes the March WWE effect, the eastward displacement of the warm pool and accompanying cooling in the western Pacific cause the displacement of the main area of deep convection (Fig. 2a) with maximum convective activity centered at 160°E.<sup>1</sup>

In order to identify the spatial scale of convection, Fig. 3 shows the distributions of OLR and SST after the rapid eastward displacement of the warm pool, that is, from mid-April to mid-May. In both REF and NWE ensemble runs, the minimum in OLR occurs north of the equator (Figs. 3b and 3c), but the distribution of convection over the warm pool is substantially different. In the NWE ensemble run, although warm waters extend to the dateline at the equator, deep convection mostly remains north of the equator with an equatorial component confined over the far western Pacific. In the REF ensemble run, warm waters are displaced eastward to 155°W and deep convection now shows a broad equatorial signature extending from 150°E to 170°W. The model results therefore demonstrate that, because of the overall warmth of the ocean in the west Pacific, modest SST anomalies can strongly perturb the convective ac-

<sup>1</sup> It is worth mentioning that these OLR anomalies consist of a negative feedback, which will tend to reduce the amplitude of the SST anomalies between the REF and NWE experiments.

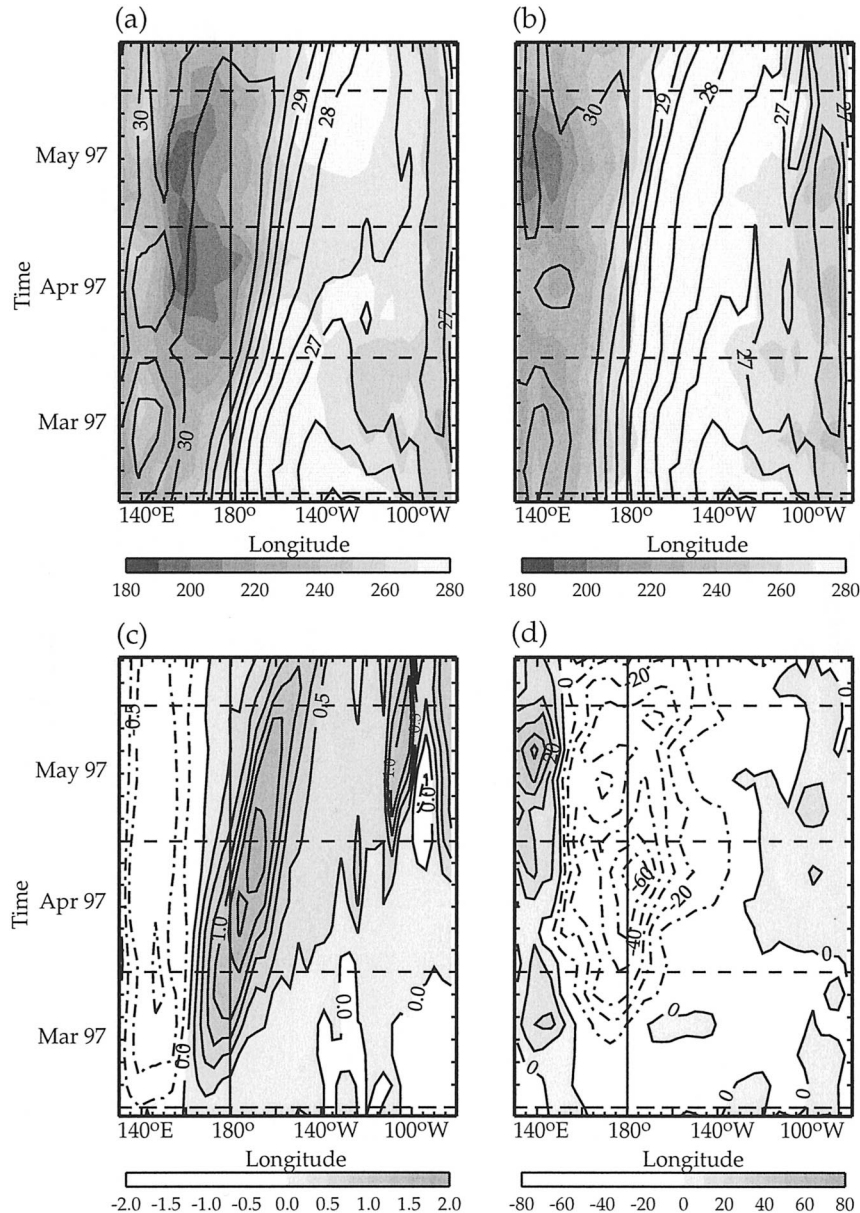


FIG. 2. Equator-time plot averaged over  $3^{\circ}N$ – $3^{\circ}S$  of OLR (shading) and SST (contours) for (a) REF ensemble mean, (b) NWE ensemble mean and for their difference REF – NWE, (c) SST, (d) OLR. Interval is  $10 W m^{-2}$  for OLR and  $0.5^{\circ}C$  for SST.

tivity over the warm pool (Fig. 3d). The response of the convection in the REF ensemble run can be compared with the observed distribution of convection (Fig. 3a). The OLR pattern agrees fairly well, although the model has overestimated the strength of the convection over the northwest equatorial Pacific, despite the use of an ensemble mean.

To demonstrate the significance and robustness of the differences between the REF and NWE experiments, the spread between the 10 members of each ensemble has been considered by taking the OLR from mid-March to mid-June, and averaging it over a region encom-

passing the EEWP (Fig. 4). The mean OLR of REF ensemble (heavy black line) decreases strongly from mid-March to mid-April as the convection responds to the eastward migration of the warm pool. Although each member shows similar trends, they exhibit large variations around the ensemble average, associated with individual weather events. In comparison, the NWE ensemble shows neither the rapid decrease in OLR in March/April, nor such large variations between ensemble members. This implies that, even in individual runs, deep convection is almost absent from this area during this time period in the NWE simulations. In fact, during

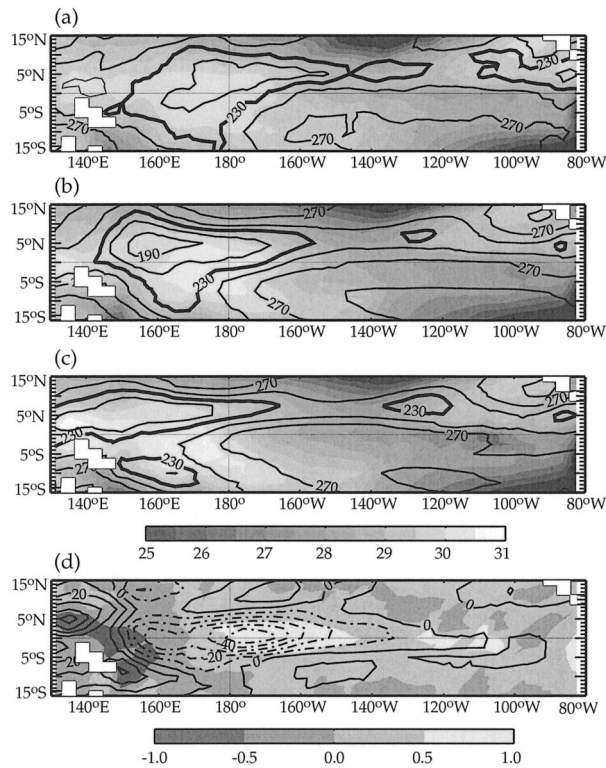


FIG. 3. SST (shading) and OLR (contours) over the tropical Pacific from mid-Apr to mid-May for (a) observations, (b) REF ensemble mean, (c) NWE ensemble mean, and (d) their difference REF – NWE. Interval is  $0.5^{\circ}\text{C}$  for SST and  $20 \text{ W m}^{-2}$  for OLR.

April and May the two distributions belonging to the REF and NWE ensembles are well separated indicating that the behavior of the convection is significantly modified by the oceanic response to the 1997 March WWE.<sup>2</sup>

The time evolution of OLR for REF ensemble around the EEWP closely matches with the observations during the three months following the March event (Fig. 4). The rapid decrease in OLR from March to April is as observed and evidence of enhanced convection (low OLR) on subseasonal timescales in April and May are found in both REF ensemble and the observations. These modeled and observed convective events display similar characteristics (intensity, duration, fetch) over the western Pacific. However, their origin is somewhat different. In the observations, the observed subseasonal convective activity over the west Pacific during boreal winter and spring is often part of large eastward-moving disturbances, originating in the Indian Ocean and commonly referred to as the Madden–Julian oscillation (MJO; Madden and Julian 1994). For example, both December 1996 and March 1997 convective events, that took place over the warm pool, were associated with MJOs (Yu and Rienecker 1998). However, observed

<sup>2</sup> Note that the two distributions converge in June because, as noted in section 2, the SST forcing converges.

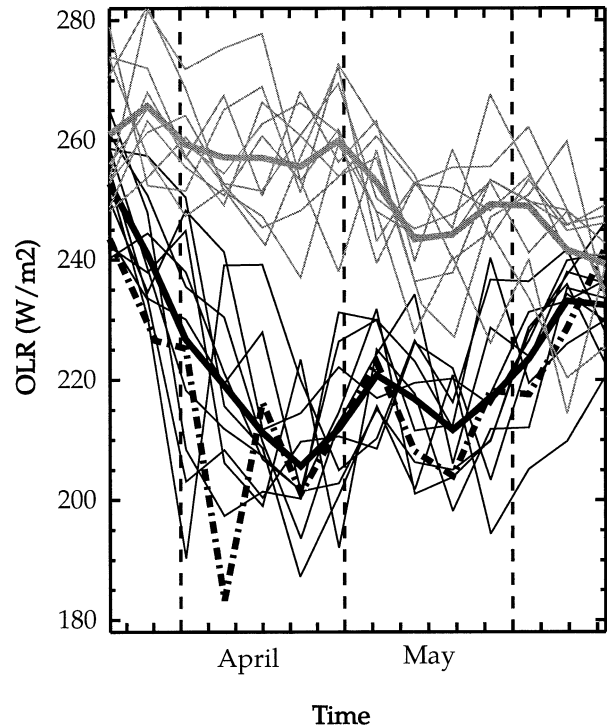


FIG. 4. Time evolution of OLR for REF ensemble mean (black thin line) and the corresponding individual runs (black dashed line), NWE ensemble mean (gray thick line) and the corresponding individual runs (gray thin lines), and the observations (black dashed line) averaged over a box  $3^{\circ}\text{N}$ – $3^{\circ}\text{S}$ ,  $160^{\circ}\text{E}$ – $170^{\circ}\text{W}$ .

events can also be associated with local processes, which seems to be the case for the April event (Slingo 1998) where the enhanced convection is a simple response to the eastward migration of the warm pool and the change in SST pattern. The model does not display such diversity in processes generating subseasonal convective events. For example, the model does not correctly reproduce the MJO: as in many AGCMs, the eastward propagation from the Indian Ocean to the west Pacific is often poorly represented (e.g., Slingo et al. 1996; Sperber et al. 1997) and the models tend to produce, at best, standing oscillations of convective activity over both areas (Inness et al. 2001). Thus, in our experiments, convective events are largely local processes, as the observed April 1997 event.

#### b. Surface wind response to the March 1997 WWE

In the previous section, the convective response to the changes in SST induced by the March 1997 WWE was described. This is, of course, accompanied by changes in the surface winds, which will in turn further affect the ocean. Although the focus of this paper is on understanding the atmospheric response to the March 1997 WWE, it is important to view this in the context of the coupled ocean–atmosphere system. Consequently the wind diagnostics will focus on the zonal component,

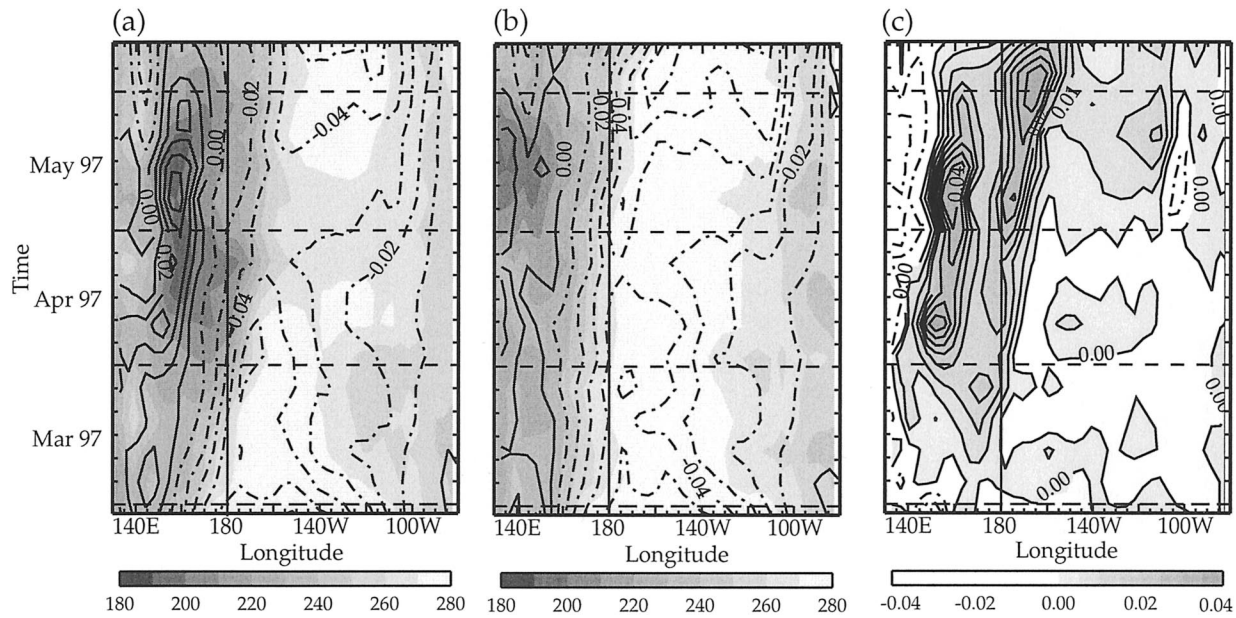


FIG. 5. Equator-time plot averaged over  $3^{\circ}\text{N}$ – $3^{\circ}\text{S}$  of OLR (shading) and zonal wind stress (contours) for (a) REF ensemble mean, (b) NWE ensemble mean, and (c) zonal wind stress for their difference REF – NWE. Interval is  $0.01 \text{ N m}^{-2}$  for zonal wind stress and  $10 \text{ W m}^{-2}$  for OLR.

which is the first order process important for forcing the ocean at intraseasonal timescales within about  $5^{\circ}$  of the equator (Battisti 1988).

Although the convective response was quite simple with enhanced convection occurring along the edge of the warm pool, the surface wind response is more complex (Fig. 5). The equatorial zonal wind stress in the NWE experiment (Fig. 5b) is typical of the normal distribution with strong easterly trades over the east Pacific and the westerlies of the Australian monsoon penetrating out to around  $150^{\circ}\text{E}$  over the west Pacific. These westerlies gradually weaken during the boreal spring to be replaced by easterlies during the Asian summer monsoon. In the REF experiment, this pattern of zonal wind stress is substantially altered. As Fig. 5c shows, there are three distinct responses by the AGCM to the SST anomalies generated by the March 1997 WWE, two of which describe a weakening of the trade winds. Over the central and eastern Pacific, east of the EEWP, a positive zonal wind stress anomaly (up to  $0.015 \text{ N m}^{-2}$ ) develops during the latter part of the integration, from  $160^{\circ}$  to  $110^{\circ}\text{W}$ . This anomaly reflects a weakening of the trade winds by more than 10% from the beginning of May to mid-June in the REF ensemble run (Fig. 5a) compared to the NWE ensemble run (Fig. 5b).

The second response is found around the date line between  $170^{\circ}\text{E}$  and  $160^{\circ}\text{W}$ . A strong westerly wind stress anomaly (up to  $0.035 \text{ N m}^{-2}$  at the beginning of June) occurs above the warm SST anomaly associated with the displacement of the EEWP (Fig. 2c). Again, this is equivalent to a reduction of the trade winds in REF compared to NWE ensemble run. This weakening

of the trades is a common feature of the El Niño growing phase, and the mechanisms that contribute to such zonal wind stress anomalies and their implications in the 1997/98 El Niño growing phase will be discussed in the next section.

The third atmospheric response occurs over the warm pool, mostly between  $150^{\circ}$  and  $170^{\circ}\text{E}$ , where another strong westerly wind stress anomaly (up to  $0.035 \text{ N m}^{-2}$ ) develops from the beginning of April to the end of May. However, in this case the westerly anomaly is collocated with the basic westerly flow, so that the wind stresses are actually enhanced in this region leading to potentially much greater forcing of the ocean. It is clear from Fig. 5a that the increased westerlies are closely linked with the enhanced convection and so can be interpreted as a dynamical response to the increase in convective activity. However, the collocation of the maxima in the surface winds and convection is a particular aspect of the model's behavior that has been noted in other studies (e.g., Inness et al. 2001, 2003). This tends not to be supported by the observations, which typically show that the maximum in convection is collocated with the maximum convergence in the surface winds, as was the case in early 1997 (Fig. 1).

As with the convection, the ensemble mean westerlies centered around  $160^{\circ}\text{E}$  in April and May for the REF experiment are constructed from a large number of westerly wind events in the individual members of the ensemble. Figure 6 displays the zonal wind stress variability over the warm pool ( $150^{\circ}$ – $170^{\circ}\text{E}$ ) for each member of REF and NWE ensembles. As already shown in Fig. 5, the REF ensemble mean zonal wind stress re-

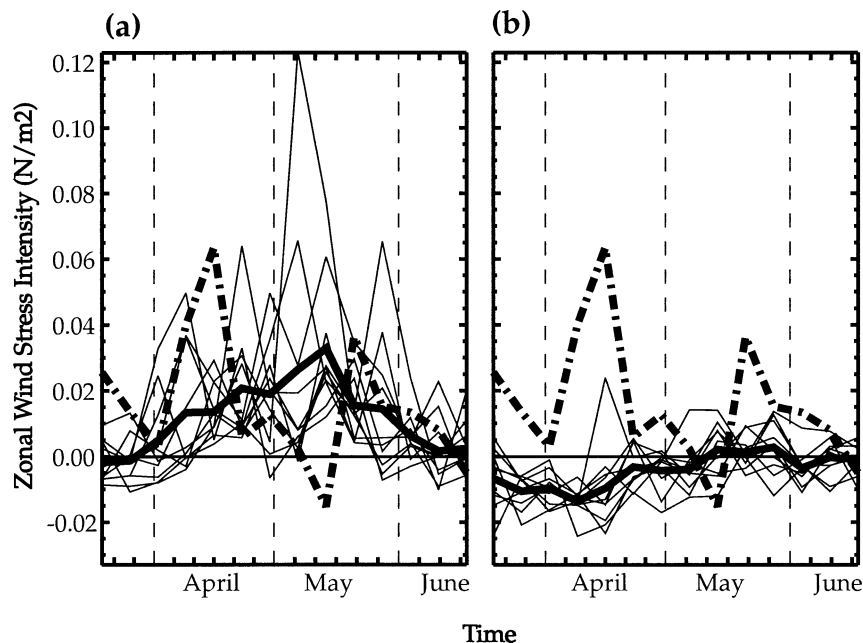


FIG. 6. (a) Time evolution of zonal wind stress averaged over a box  $3^{\circ}\text{N}$ – $3^{\circ}\text{S}$ ,  $150^{\circ}$ – $170^{\circ}\text{E}$  for REF ensemble mean (black thick line), the observation (black dotted line), and each individual run of the REF ensemble (black thin lines). (b) Same as (a) but for NWE ensemble run.

mains positive during the three months following the strong March wind event (Fig. 6a), whereas NWE mean zonal wind stress is mostly negative over the period (Fig. 6b). Moreover, the high-frequency variability (7–30 days) is clearly stronger in the REF ensemble, each member displaying energetic westerly wind events of varying duration and intensity from April to June. In contrast, the standard deviation of the zonal wind stress in the NWE ensemble is weak and no intense WWEs occur. Again as with the convective variability (Fig. 4), the two distributions are well separated suggesting that the enhanced wind variability in the REF experiment is a direct consequence of the different SST forcing. The characteristics of the wind variability in the REF ensemble are also much nearer the observed with WWEs of similar amplitude.

Finally, to draw a more quantitative view of the WWEs in each ensemble, a WWE classification is shown in Table 1. To that end, we define WWEs as follows: any period of westerly wind stress (average

between  $3^{\circ}\text{N}$  and  $3^{\circ}\text{S}$ ) from  $130^{\circ}\text{E}$  to  $150^{\circ}\text{W}$  whose maximum intensity is greater than  $0.02 \text{ N m}^{-2}$  is considered a WWE. The duration of all these events ranges from one to three weeks and their zonal fetch range between  $5^{\circ}$  and  $30^{\circ}$  with a positive correlation between fetch and intensity. These criteria are more restrictive than the one used by Harrison and Vecchi (1997), so that only those WWEs are selected that can potentially have a large oceanic impact by forcing equatorial downwelling Kelvin waves, contributors to the onset of El Niño (McPhaden 1999; Boulanger and Menkes 1999; Slingo and Delecluse 1999). We then define three types of WWEs relative to their intensity: type I ( $0.02 \text{ N m}^{-2} < \tau_x < 0.05 \text{ N m}^{-2}$ ), type II ( $0.05 \text{ N m}^{-2} < \tau_x < 0.08 \text{ N m}^{-2}$ ), and type III ( $\tau_x > 0.08 \text{ N m}^{-2}$ ). Based on this procedure, 30 WWEs occurred during April–May among the 10 members of REF ensemble run, that is, 3 WWEs per run on average (Table 1). By contrast, only nine events occurred in the NWE ensemble run, mostly located over the far western Pacific (west of  $150^{\circ}\text{E}$ ). Moreover, REF WWEs displayed a broad range of intensity, whereas all NWE WWEs are weak and always fall in category I. The two groups of WWEs (REF and NWE) represent two distinct ensembles, which are well separated statistically at the 1% significance level (see appendix). Thus, the REF ensemble produces much stronger WWE activity over the warm pool, from which it can be concluded that the SST anomalies forced by the March 1997 WWE had a major impact on the generation of subsequent westerly wind activity over the warm pool, as the El Niño developed.

TABLE 1. Total number, number in category I (weak), II (moderate), and III (strong), mean intensity and standard deviation for WWEs in REF, NWE, and NWC ensemble runs.

	No. of WWE	No. of WWE in I	No. of WWE in II	No. of WWE in III	Mean WWE intensity ( $\text{N m}^{-2}$ )	Std dev ( $\text{N m}^{-2}$ )
REF	30	12	12	6	0.064	0.044
NWE	9	9	0	0	0.032	0.011
NWC	24	16	8	0	0.040	0.017

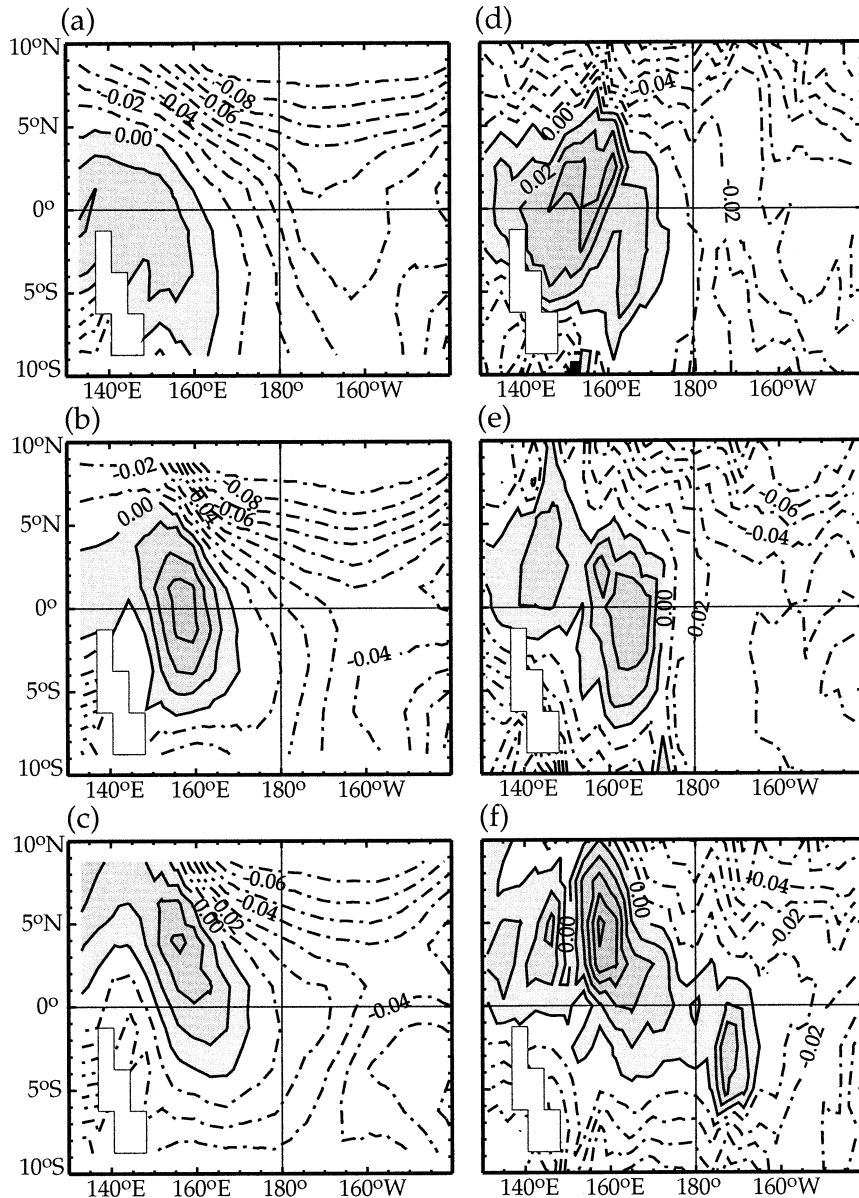


FIG. 7. Zonal wind stress (shading) over the western tropical Pacific from (a), (d) mid-Mar to mid-Apr, (b), (e) mid-Apr to mid-May, and (c), (f) mid-May to mid-Jun. The REF ensemble mean is in (a)–(c) and the observations are in (d)–(f). Interval is  $0.01 \text{ N m}^{-2}$ .

As well as the temporal characteristics of the wind stress variability in the REF ensemble, the spatial patterns of the wind stress anomalies also compare favorably with observations during the three months following the March event (Fig. 7). Allowing for the smoothness of the REF ensemble mean winds, the eastward propagation of the region of westerlies in April between  $150^\circ$  and  $170^\circ\text{E}$  is well captured by the model (Figs. 7b and 7e and Fig. 3). The spatial structures are also comparable. Both are centered on the equator with a latitudinal and longitudinal fetch of about  $10^\circ$ . During June (Figs. 7c and 7f), westerlies occur north of the equator (at about  $4^\circ\text{N}$ ) in both the observations and the model,

again with comparable fetches. These results suggest that the structure and location of westerly wind activity are determined, at least partially, by the boundary conditions and the large-scale flow over the western Pacific.

#### 4. Discussion

##### a. The reduction in the trade winds

As described in the previous section, a notable feature of the atmospheric response to the SST anomalies generated by the March WWE consisted of a weakening of the trade winds over the central and eastern Pacific.

There are two distinct aspects to this wind response. The first one is a 10%–20% weakening of the trade winds east of 160°W, along the path of the ocean Kelvin wave. Two explanations can be put forward to explain this. The first one is associated with the large-scale changes in atmospheric convection. Following the March WWE, the tropical western Pacific heat source associated with lower-tropospheric convergence and ascending motion, moves eastward (Fig. 2a). This eastward movement represents a weakening of the Pacific-wide Walker circulation, which could then weaken the lower-tropospheric equatorial easterly trade winds (the lower branch of east–west air–sea exchange in the Walker cell; Neelin et al. 1998; Wang 2002). The second explanation is a more local process. The Kelvin wave generated by the March WWE produces a warming of the SST in the central eastern Pacific. The consequence of this warming is a weakening of the zonal SST gradient in this region (Figs. 2a and 2b), a major factor in driving the equatorial easterlies. The weaker zonal SST gradients from 160°W to the eastern Pacific in the REF experiment could feed back to the atmosphere by weakening the background easterlies in this region.

To determine the respective contribution of these two processes in the reduction of the trade winds, a sensitivity ensemble experiment was performed. This ensemble (named hereafter NKW) is similar to the REF ensemble except that the SST boundary conditions have been modified to remove the warming associated with the Kelvin wave path east of the EEWP (defined as the 28.5°C isoline). The NKW SSTs are now identical to the NWE SSTs in the central and eastern Pacific east of the 28.5°C isoline. The impact of removing these warm SST anomalies on evolution of the trade winds in the central eastern Pacific is presented in Fig. 8 for REF, NWE, and NKW ensemble means. While the weakening of the trade winds is clearly evident for REF ensemble (compared to NWE), no weakening occurs for NKW ensemble. On the other hand, since the REF and NKW SSTs are identical in the western Pacific, the eastward convection shift also occurs in the NKW ensemble run (not shown). These results therefore provide conclusive evidence that the weakening of the zonal SST gradients in the central eastern Pacific, as a result of the downwelling ocean Kelvin wave generated by the March WWE, is largely responsible for the reduction in the easterly trades.

The second contribution in the overall weakening of the trade winds involves the development of a strong westerly wind anomaly following the displacement of the EEWP. Such an atmospheric pattern can be interpreted in terms of a surface wind response to the positive SST anomaly. The question of what drives surface winds is largely a question of what influences surface pressure gradients. Two thermal influences on surface pressure are usually considered: forcing by the hydrostatic pressure anomalies in the boundary layer induced by the SST anomalies themselves (Lindzen and Nigam

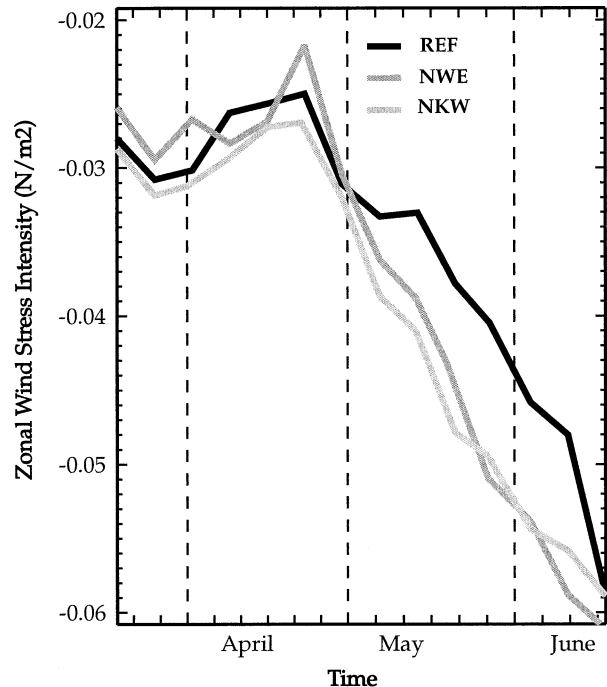


FIG. 8. Time evolution of zonal wind stress averaged over a box 3°N–3°S, 160°–100°W for REF ensemble mean (black thick line), NWE ensemble mean (gray thick line), and NKW ensemble mean (gray dashed line).

1987) and thermal forcing from cloud base to the tropopause by anomalous cumulus convection. Because these mechanisms are highly interrelated, it has not been clearly demonstrated how much each mechanism contributes to the surface wind. In a recent series of papers, Wu et al. (1999, 2000, and 2001) demonstrated that the contribution from the surface pressure gradient versus thermal forcing is mostly controlled by the relative importance of Newtonian cooling and Rayleigh friction. They argue that significant surface wind anomalies can be driven by an elevated heat source only when Newtonian cooling dominates: in this case only, thermal damping is able to homogenize the atmospheric motion in the vertical direction and to generate a strong vertically uniform wind below the bottom of the heat source. Chiang et al. (2001) attempts to address the question of how each forcing-elevated heating and surface temperature gradient relates to anomalous surface winds in the Tropics using a linear primitive equation model with idealized parameterizations for the two forcings. They concluded that it is upper-level heating that drives surface wind but they parameterized boundary layer cooling in such a manner that it was equivalent to a very strong Newtonian cooling. Their results also underline that the surface wind response to elevated heating is very sensitive to the thermal relaxation rate of the planetary boundary layer. Further investigations are therefore needed with realistic parameterizations to address this key issue.

This weakening of the trade winds along the path of the Kelvin wave as well as along the EEWP displacement could be of paramount importance for the evolution of El Niño. They act as a positive feedback on the coupled system in potentially two ways. The weakening of the easterlies along the displaced EEWP will generate further downwelling Kelvin waves, which act to deepen the thermocline in the central and eastern Pacific, while the westerly wind anomalies in the eastern Pacific will reduce the equatorial upwelling, so limiting the amount of cold water brought to the surface. This will further increase the SST in the equatorial eastern and central Pacific, which in turn will weaken the zonal SST gradients even further.

#### *b. High-frequency winds over the western Pacific*

The other striking result of this study is the occurrence of intense and frequent deep convective events and associated WWEs over the extended warm pool in the REF ensemble during the months following the March event. This implies that the oceanic impact of the March WWE set in place the conditions required to reproduce the observed surface wind variability that occurred after March 1997, during the onset phase of the 1997/98 El Niño. This variability over the warm pool is of paramount importance in determining the timing and the growth rate of an El Niño event. In fact, these WWEs generate intense eastward currents at the surface that are likely to advect the warm pool farther east, enhancing the eastward shift of convective activity and the concurrent development of westerly wind anomalies in the central Pacific (Picaut et al. 1996). Moreover, it has been shown that these WWEs during April and May warm the eastern Pacific SST two or three months later through the generation of downwelling equatorial Kelvin waves, increasing the Niño-3 (5°S–5°N, 150°–90°W) SST anomaly by about 0.5°C (van Oldenborgh 2000). The WWEs represent, therefore, a fundamental process for the EEWP displacement and for the maintenance of the central eastern Pacific SST anomalies during the development stage of El Niño.

The amount of momentum transferred from the atmosphere to the ocean, and therefore the growth rate of the El Niño event, strongly depends on the intensity of the westerly wind anomalies in the western Pacific during the onset and development stage (Federov 2002). Even though the occurrence of these WWEs seems to be strongly influenced by the oceanic impact of the March 1997 event, the processes that control their intensity are not fully understood. Some studies have provided a classification of the WWEs that occur over the western Pacific in terms of intensity, duration, and fetch (Keen 1982; Giese and Harrison 1991; Harrison and Vecchi 1997), but the physical processes controlling these characteristics are still unclear. In fact, in the observations, westerly wind event occurrences and characteristics are connected with a variety of atmospheric

conditions: paired and individual tropical cyclones (McBride et al. 1995; Hartten 1996), cold surges from midlatitudes (Chu 1988; Chu and Frederick 1990), convective episodes associated with the passage of the active phase of the Madden–Julian oscillation (Lin and Johnson 1996), or a combination of all three. For instance, Yu and Rienecker (1998) suggest that the background for the December 1996 and March 1997 WWEs was set by the MJO but that enhancement process was largely triggered by cold surges and twin cyclones. In the following, we want to explore the influence of the SST structure over the western Pacific on the characteristics of the WWEs. To that end, another sensitivity ensemble run (named hereafter NWC) has been performed. It is identical to the REF ensemble run except that the SST cooling generated by the March event in the far western Pacific has been removed. This sensitivity experiment allows us to test whether a modest change in the SST distribution over the warm pool would constrain the WWEs characteristics or if these characteristics are only determined by the atmospheric large-scale flow over the western Pacific.

The impact of removing the far western Pacific cooling on the OLR and the zonal surface wind stress is presented in Fig. 9. As in the REF ensemble, convection develops over the central Pacific in association with the eastward displacement of the warm pool (Fig. 9a), although the convective response is not as strong (cf. Fig. 2a). Again this can be interpreted in terms of the response by the convection to changes in the zonal SST gradient. The removal of the far western Pacific cooling has substantially weakened the SST gradients on the western edge of the warm pool leading to a weakening of the westerly winds, which feed the convection. In fact, the most striking differences between the two ensembles are in the surface wind stress field. The positive zonal wind stress pattern between 150° and 170°E in the REF ensemble is nearly halved in the NWC ensemble.

As in the NWE ensemble, the reduced westerly wind stress in the NWC ensemble is characterized by a weakening of the WWEs occurring over the western Pacific during the months following the March event (Table 1). The total number of WWEs is somewhat lower (24 in NWC compared to 30 in REF), but their mean intensity has decreased substantially. There are no strong WWEs (category III) and fewer moderate WWEs (category II) in the NWC ensemble compared to the REF ensemble. Differences in the distribution of WWEs in the two ensembles (REF and NWC) are significant at the 1% significance level (see the appendix). This result underlines the strong dependence of the characteristics of WWEs on the SST structure over the warm pool.

## 5. Summary and conclusions

Our overall objective is to understand the role of the March 1997 WWE in the onset of the 1997/98 El Niño.

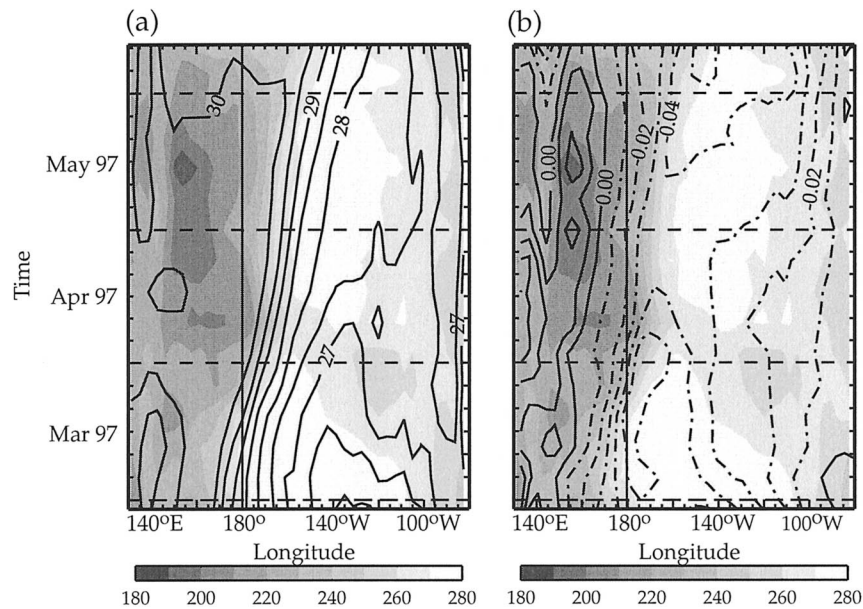


FIG. 9. Equator-time plot averaged over  $3^{\circ}\text{N}$ – $3^{\circ}\text{S}$  for NWC ensemble mean of (a) OLR (shading) and SST (contours) and (b) OLR (shading) and zonal wind stress (contours). Interval is  $10 \text{ W m}^{-2}$  for OLR,  $0.5^{\circ}\text{C}$  for SST and  $0.01 \text{ N m}^{-2}$  for zonal wind stress.

To reach that goal, we first examined the *oceanic* response to this WWE (Lengaigne et al. 2002). This highlighted three major responses: (i) a cooling of the far western Pacific ( $\sim 0.8^{\circ}\text{C}$ ), (ii) a rapid eastward displacement of the eastern edge of the warm pool (2000 km in a month), and (iii) a weak warming of the central eastern Pacific along the Kelvin wave path ( $\sim 0.5^{\circ}\text{C}$ ). Based on these results, the present study investigated the *atmospheric* response to each of these oceanic impacts in order to suggest potential positive feedback loops, which may have been responsible for the onset and rapid growing rate of the 1997/98 El Niño. In a subsequent paper the fully coupled response will be explored.

The results of the sensitivity experiments described in this paper suggest that the three major oceanic anomalies generated by the March 1997 WWE initiated two basic atmospheric responses, both of which favored a rapid growth toward El Niño conditions. First, there was a weakening of the equatorial easterly trade winds, which arose for two different reasons. The rapid eastward displacement of the eastern edge of the warm pool strongly reduced the trade winds near the date line while the central eastern Pacific warming, along the forced oceanic Kelvin wave path, decreased the east–west SST temperature gradient resulting in a weakening (10%–20%) of the trade wind intensity in the central eastern Pacific.

The second major atmospheric response to the March 1997 WWE occurs over the warm pool. The eastward displacement of the warmest water from the western to the central Pacific during the two months following the wind event induced an eastward shift of convection and

promoted the occurrence of frequent and intense WWEs in April and May. The reduction of the trade winds, together with the occurrence of these strong WWEs, are likely to reinforce the initial equatorial Pacific warming first through a reduction of the upwelling and second through the advection of warmer water (van Oldenborgh 2000; Boulanger and Menkes 2001; Vialard et al. 2001).

The results of this study provide compelling evidence that, in certain conditions, such as the onset of the 1997/98 El Niño, a single, strong WWE (such as the March 1997) can strongly influence the El Niño growth rate, not only by its direct oceanic impact (in this case, warm pool displacement, central and eastern Pacific warming), but also by its atmospheric positive feedback (trade winds weakening and generation of strong WWEs during the following months). It must however be kept in mind that this WWE was embedded in a sequence of MJOs, and that its intensity likely benefited from the SST changes produced by prior WWEs (i.e., the December 1996 one), as well as low-frequency oceanic precursors.

Confirmation of the potential for WWEs to influence strongly the onset and development stage of El Niño has been provided, indirectly, by the predictions of the 1997/98 El Niño. Most of the forecasts, with the exception of ECMWF, failed to capture the onset of the El Niño prior to the March WWE, and it was not until after June that the forecasts managed to represent the intensity of the event at a time when the El Niño was already very strong (Barnston et al. 1999). In particular, no model predicted the extremely steep rise of the central and eastern Pacific SSTs that took place in March–June 1997. These shortcomings may be attributed to the

fact that most of these models do not simulate well, if at all, WWEs and their associated atmospheric causes (e.g., MJO, tropical cyclones; see Slingo et al. 1996).

It could be argued, therefore, that WWEs (and possibly more general high-frequency wind variability) seem to modulate strongly the onset and development stage of El Niño through coupled feedbacks. This may be one of the main reasons for irregularity in the ENSO cycle in terms of evolution, amplitude, and frequency, something that many coupled models have difficulty in simulating (Achutarao et al. 2002). Unfortunately, the interannual and intraseasonal variability of these wind events remains, at the moment, largely unpredictable. In fact, the occurrence and characteristics of WWEs are connected with a variety of atmospheric circulation conditions: paired and individual tropical cyclones, convective episodes associated with the passage of MJO active phase, cold surges from midlatitudes, or a combination of the three. This complexity strongly limits their predictability and could therefore also place limitations on the long lead-time predictions of El Niño. For shorter lead times however, the results of this study suggest that there is cause for optimism. Although the March 1997 WWE may not have been correctly simulated by the model, the SST anomalies generated by the March event are sufficient to constrain the wind variability in the following months. This variability, an essential feature of the 1997/98 El Niño (van Oldenborgh 2000), is therefore not unpredictable weather noise but an indirect consequence of the March event. Moreover, the intensity and/or the structure of the WWEs seems to be highly dependent on the SST characteristics over the western Pacific: a moderate warming of the far western Pacific induces a weakening of the WWE intensity in April–May. Therefore, not only the location of the eastern edge of the warm pool but also the SST structure, mostly via its gradient, are essential to determine the characteristics of the WWEs. Further observations analyses are under way to validate these model results.

The model's inability to simulate the March 1997 WWE is linked to its inability to correctly reproduce the MJO, which was one of the main causes of the exceptional intensity of this event (Yu and Rienecker 1998). Even if some WWEs are of synoptic scales (smaller than those of the MJO in both time and space), a large part of them (often the most intense) are associated with MJO. Maintaining realistic MJO signals in ENSO forecast models is therefore essential to improve skills of ENSO prediction. But it is a difficult endeavor: dynamic models do not have any skill predicting MJO beyond a few days (Hendon et al. 2000) and the mechanisms responsible for producing the marked interannual fluctuations in MJO activity remains unclear (Slingo et al. 1999; Hendon et al. 1999; Bergman et al. 2001). Nevertheless, numerous studies have helped to understand better the physical mechanisms involved in the MJO (Woolnough et al. 2001; Inness and Slingo 2003;

Inness et al. 2003) and we can therefore expect improvements in the representation of this phenomenon in coupled models. However, the associated surface wind stress variability and more particularly the WWE's structure and intensity, which depends on the characteristics of the large-scale MJO as well as on the SST structure of the western warm pool, cold surge, and synoptic processes, will certainly remain difficult to predict.

All these results have been obtained using an atmospheric only model and further fully coupled experiments are planned to confirm the coupled mechanisms at work during the onset of El Niño. Unfortunately, most of the existing coupled models do not simulate a sufficiently realistic basic state over the western warm pool to allow us to investigate the coupled mechanisms suggested by our study. Indeed, the trade winds extend too far over the western Pacific, the warm pool is often eroded and WWEs mostly occur over the Maritime Continent. Further improvements of these models are under way, which will then provide the basis for a better understanding of high-frequency ocean–atmosphere coupling that could interact constructively with the ENSO cycle. This should therefore improve our ability to simulate and predict the timing and amplitude of future El Niños.

*Acknowledgments.* This work was supported by the Programme National d'Etude du Climat. Computations were carried out at CSAR, Manchester and at the IDRIS/CNRS, Paris. Matthieu Lengaigne gratefully acknowledges the computing support of Jeff Cole during several fruitful visits at the CGAM, Reading. He also would further like to thank Pete Inness and Pascal Terray for fruitful discussions and the two anonymous reviewers for their comments.

## APPENDIX

### The Mann–Whitney Test

The Mann–Whitney test is a nonparametric procedure that is a powerful tool for testing the hypothesis that two sample populations ( $X$  and  $Y$ ) have the same mean of distribution against the hypothesis that they differ. The test is derived by examining the probability distribution of a linear combination of the ranks of the population under the null hypothesis that all the values are sampled from the same continuous distribution.

The procedure ranks the population's values from smallest to largest, assigning the rank 1 to the smallest observation, 2 to the next largest, and so on up to rank  $n$ , the number of elements in the two populations. Then, the Mann–Whitney statistics for  $X$  and  $Y$  are defined as follows:

$$U(X) = n_x n_y + n_x(n_x + 1)/2 - W_x$$

$$U(Y) = n_x n_y + n_y(n_y + 1)/2 - W_y,$$

where  $n_x$  and  $n_y$  are the number of elements in  $X$  and  $Y$ , respectively, and  $W_x$  and  $W_y$  are the rank sums for  $X$  and  $Y$ . The test statistic  $Z$ , which closely follows a normal distribution for sample sizes exceeding 10 elements, is defined as follows:

$$Z = \frac{U_x - (n_x n_y)/2}{\sqrt{[n_x n_y (n_x + 1)]/12}}.$$

When this probability level is sufficiently small, we reject the null hypothesis and conclude that the two sample populations do not come from the same distribution.

#### REFERENCES

- Achutarao, K., K. R. Sperber, and the CMIP modelling groups, 2002: Simulation of the El Niño Southern Oscillation: Results from the Coupled Model Intercomparison Project. *Climate Dyn.*, **19**, 191–209.
- Barnston, A. G., M. H. Glantz, and Y. He, 1999: Predictive skill of statistical and dynamical climate models in SST forecasts during the 1997–98 El Niño episode and the 1998 La Niña onset. *Bull. Amer. Meteor. Soc.*, **80**, 217–243.
- Battisti, D. S., 1988: Dynamics and thermodynamics of a warming event in a coupled tropical atmosphere–ocean model. *J. Atmos. Sci.*, **45**, 2889–2919.
- Bentamy, A., Y. Quilfen, F. Gohin, N. Grima, M. Lenaour, and J. Servain, 1996: Determination and validation of average wind fields from ERS-1 scatterometer measurements. *Global Atmos. Ocean Syst.*, **4**, 1–29.
- Bergman, J. W., H. H. Hendon, and K. M. Weickmann, 2001: Intra-seasonal air–sea interactions at the onset of El Niño. *J. Climate*, **14**, 1702–1719.
- Boulanger, J.-P., and C. Menkes, 1999: Long equatorial wave reflection in the Pacific Ocean from TOPEX/Poseidon data during the 1992–1998 period. *Climate Dyn.*, **15**, 205–225.
- , and —, 2001: The Trident Pacific model. Part 2: Role of long equatorial wave reflection on sea surface temperature anomalies during the 1993–1998 TOPEX/Poseidon period. *Climate Dyn.*, **17**, 175–186.
- Chiang, J. C. H., S. E. Zebiak, and M. A. Cane, 2001: Relative roles of elevated heating and surface temperature gradients in driving anomalous surface winds over tropical oceans. *J. Atmos. Sci.*, **58**, 1371–1394.
- Chu, P. S., 1988: Extratropical forcing and the burst of equatorial westerlies in the western Pacific: A synoptic study. *J. Meteor. Soc. Japan*, **66**, 549–564.
- , and J. Frederick, 1990: Westerly wind bursts and surface heat fluxes in the equatorial western Pacific in May 1982. *J. Meteor. Soc. Japan*, **68**, 523–536.
- Fedorov, A. V., 2002: The response of the coupled tropical ocean–atmosphere to westerly wind bursts. *Quart. J. Roy. Meteor. Soc.*, **128**, 1–23.
- Giese, B. S., and D. E. Harrison, 1991: Eastern equatorial Pacific response to three composite westerly wind types. *J. Geophys. Res.*, **96** (Suppl.), 3239–3248.
- Gregory, D., and P. R. Rowntree, 1990: A mass flux convection scheme with the representation of cloud ensemble characteristics and stability dependent closure. *Mon. Wea. Rev.*, **118**, 1483–1506.
- , and S. Allen, 1991: The effect of convective scale downdrafts upon NWP and climate simulations. Preprints, *Ninth Conf. on Numerical Weather Prediction*, Denver, CO, Amer. Meteor. Soc., 122–123.
- , R. Kershaw, and P. M. Inness, 1997: Parametrisation of momentum transport by convection. II: Tests in single column and general circulation models. *Quart. J. Roy. Meteor. Soc.*, **123**, 1153–1183.
- Harrison, D. E., and G. Vecchi, 1997: Westerly wind events in the tropical Pacific, 1986–1995. *J. Climate*, **10**, 3131–3156.
- Hartten, L. M., 1996: Synoptic settings of westerly wind bursts. *J. Geophys. Res.*, **101**, 16 997–17 019.
- Hendon, H. H., C. Zhang, and J. D. Glick, 1999: Interannual variability of the Madden–Julian oscillation during austral summer. *J. Climate*, **12**, 2538–2550.
- , B. Liebmann, M. Newman, J. D. Glick, and J. E. Schemm, 2000: Medium-range forecast errors associated with active episodes of the Madden–Julian oscillation. *Mon. Wea. Rev.*, **128**, 69–86.
- Inness, P. M., and D. Gregory, 1997: Aspects of the intraseasonal oscillation simulated by the Hadley Centre Atmosphere Model. *Climate Dyn.*, **13**, 441–458.
- , and J. M. Slingo, 2003: Simulation of the Madden–Julian oscillation in a coupled general circulation model. Part II: The role of the basic state. *J. Climate*, **16**, 365–382.
- , —, S. J. Woolnough, R. B. Neale, and V. D. Pope, 2001: Organization of tropical convection in a GCM with varying vertical resolution: Implications for the simulation of the Madden–Julian oscillation. *Climate Dyn.*, **17**, 777–793.
- , —, E. Guilyardi, and J. Cole, 2003: Simulation of the Madden–Julian oscillation in a coupled general circulation model. Part I: The importance of atmosphere–only interaction. *J. Climate*, **16**, 345–364.
- Keen, R. A., 1982: The role of cross-equatorial cyclone pairs in the Southern Oscillation. *Mon. Wea. Rev.*, **110**, 1405–1416.
- Kessler, W. S., and R. Kleeman, 2000: Rectification of the Madden–Julian oscillation into the ENSO cycle. *J. Climate*, **13**, 3560–3575.
- , M. J. McPhaden, and K. M. Weickmann, 1995: Forcing of intraseasonal Kelvin waves in the equatorial Pacific. *J. Geophys. Res.*, **100**, 613–631.
- Kleeman, R., and A. M. Moore, 1997: A theory for the limitation of ENSO predictability due to stochastic atmospheric transients. *J. Atmos. Sci.*, **54**, 753–767.
- Lau, K.-M., and P. H. Chan, 1986: The 40–50 day oscillation and the El Niño/Southern Oscillation: A new perspective. *Bull. Amer. Meteor. Soc.*, **67**, 533–534.
- Lengaigne, M., J.-P. Boulanger, C. Menkes, S. Masson, G. Madec, and P. Delecluse, 2002: Ocean response to the March 1997 Westerly Wind Event. *J. Geophys. Res.*, **107**, 8015, doi:10.29/2001JC000841.
- Liebmann, B., and C. A. Smith, 1996: Description of a complete (interpolated) outgoing longwave radiation dataset. *Bull. Amer. Meteor. Soc.*, **77**, 1275–1277.
- Lin, X., and R. H. Johnson, 1996: Kinematic and thermodynamic characteristics of the flow over the western Pacific warm pool during TOGA COARE. *J. Atmos. Sci.*, **53**, 695–715.
- Lindzen, R. S., and S. Nigam, 1987: On the role of sea surface temperature gradients in forcing low-level winds and convergence in the Tropics. *J. Atmos. Sci.*, **44**, 2418–2436.
- Madden, R. A., and P. R. Julian, 1994: Observations of the 40–50-day tropical oscillation—A review. *Mon. Wea. Rev.*, **122**, 814–837.
- Madec, G., P. Delecluse, M. Imbard, and C. Lévy, 1998: OPA 8.1 Ocean General Circulation Model reference manual. Note du Pôle de modélisation No.11, Institut Pierre-Simon Laplace, 91 pp.
- Matsuurra, M., and S. Iizuka, 2000: Zonal migration of the Pacific warm-pool tongue during El Niño events. *J. Phys. Oceanogr.*, **30**, 1582–1600.
- McBride, J. L., N. E. Davidson, K. Puri, and G. C. Tyrell, 1995: The flow during TOGA COARE as diagnosed by the BMRC Tropical Analysis and Prediction System. *Mon. Wea. Rev.*, **123**, 717–736.
- McPhaden, M. J., 1999: Genesis and evolution of the 1997–1998 El Niño. *Science*, **283**, 950–954.
- , and X. Yu, 1999: Equatorial waves and the 1997–98 El Niño. *Geophys. Res. Lett.*, **26**, 2961–2964.
- Neelin, J. D., D. S. Battisti, A. C. Hirst, F.-F. Jin, Y. Wakata, T.

- Yamagata, and S. E. Zebiak, 1998: ENSO theory. *J. Geophys. Res.*, **103**, 14 261–14 290.
- Picaut, J., M. Ioualalen, C. Menkes, T. Delcroix, and M. J. McPhaden, 1996: Mechanism of the zonal displacements of the Pacific warm pool: Implications for ENSO. *Science*, **274**, 1486–1489.
- Pope, V. D., M. L. Gallani, P. R. Rowntree, and R. A. Stratton, 2000: The impact of new physical parameterisations in the Hadley Centre climate model—HadAM3. *Climate Dyn.*, **16**, 123–146.
- Reynolds, R. W., and T. M. Smith, 1994: Improved global sea surface temperature analyses using optimum interpolation. *J. Climate*, **7**, 1195–1202.
- Slingo, J. M., 1998: The 1997/98 El Niño. *Weather*, **53**, 274–281.
- , and P. Delecluse, 1999: Scale interactions and the tropical atmosphere–ocean system. World Climate Research Programme Rep. WCRP-107, 416 pp.
- , and Coauthors, 1996: Intraseasonal oscillations in 15 atmospheric general circulation models: Results from AMIP diagnostic subproject. *Climate Dyn.*, **12**, 325–357.
- , D. P. Rowell, K. R. Sperber, and F. Nortley, 1999: On the predictability of the interannual behaviour of the Madden–Julian oscillation and its relationship with El Niño. *Quart. J. Roy. Meteor. Soc.*, **125**, 583–609.
- Spencer, H., and J. M. Slingo, 2003: The simulation of peak and delayed ENSO teleconnections. *J. Climate*, **16**, 1757–1774.
- Sperber, K. R., J. M. Slingo, P. M. Inness, and W. K.-M. Lau, 1997: On the maintenance and initiation of the intraseasonal oscillation in the NCEP/NCAR reanalysis and in the GLA and UKMO AMIP simulations. *Climate Dyn.*, **13**, 769–795.
- van Oldenborgh, G. J., 2000: What caused the onset of the 1997–1998 El Niño? *Mon. Wea. Rev.*, **128**, 2601–2607.
- Vialard, J., C. Menkes, J.-P. Boulanger, P. Delecluse, E. Guilyardi, M. J. McPhaden, and G. Madec, 2001: Oceanic mechanisms driving the SST during the 1997–1998 El Niño. *J. Phys. Oceanogr.*, **31**, 1649–1675.
- Wang, C., 2002: Atmospheric circulation cells associated with the El Niño–Southern Oscillation. *J. Climate*, **15**, 399–419.
- Woolnough, S. J., J. M. Slingo, and B. J. Hoskins, 2001: The organisation of tropical convection by intraseasonal sea surface temperature anomalies. *Quart. J. Roy. Meteor. Soc.*, **127**, 887–907.
- Wu, Z., E. S. Sarachik, and D. S. Battisti, 1999: Thermally forced surface winds on an equatorial beta plane. *J. Atmos. Sci.*, **56**, 2029–2037.
- , D. S. Battisti, and E. S. Sarachik, 2000: Rayleigh friction, newtonian Cooling, and the linear response to steady tropical heating. *J. Atmos. Sci.*, **57**, 1937–1957.
- , E. S. Sarachik, and D. S. Battisti, 2001: Thermally driven tropical circulations under Rayleigh friction and Newtonian cooling: Analytic solutions. *J. Atmos. Sci.*, **58**, 724–741.
- Wyrtki, K., 1985: Water displacements in the Pacific and the genesis of El Niño cycles. *J. Geophys. Res.*, **91**, 7129–7132.
- Yu, L., and M. M. Rienecker, 1998: Evidence of an extratropical atmospheric influence during the onset of the 1997–98 El Niño. *Geophys. Res. Lett.*, **25**, 3537–3540.